Abedi, Mohsen; Dowhuszko, Alexis A.; Wichman, Risto

Visible Light Communications: A Novel Indoor Network Planning Approach

Published in:
2021 IEEE Global Communications Conference, GLOBECOM 2021 - Proceedings

DOI:
10.1109/GLOBECOM46510.2021.9685571

Published: 01/01/2021

Document Version
Peer-reviewed accepted author manuscript, also known as Final accepted manuscript or Post-print

Please cite the original version:
Abedi, M., Dowhuszko, A. A., & Wichman, R. (2021). Visible Light Communications: A Novel Indoor Network Planning Approach. In *2021 IEEE Global Communications Conference, GLOBECOM 2021 - Proceedings* IEEE. https://doi.org/10.1109/GLOBECOM46510.2021.9685571

Visible Light Communications: A Novel Indoor Network Planning Approach

Mohsen Abedi, Alexis A. Dowhuszko, *Senior Member, IEEE*, and Risto Wichman
School of Electrical Engineering, Aalto University, 02150 Espoo, Finland
E-mails: {mohsen.abedi, alexis.dowhuszko, risto.wichman}@aalto.fi

***Abstract*—We propose a *Partition-based Visibility (PV) graph modeling* to find the minimum number of Visible Light Communications (VLC) nodes and their locations for reliable indoor coverage. VLC network offers a low-cost technology on a license-free spectrum to complement the contemporary mobile network services offered on Radio Frequency (RF) bands. However, VLC suffers from propagation limits: Firstly, in presence of opaque obstacles such as walls, doors, and even curtains, strong link blockage is experienced as the power of reflections is much weaker than the power of the Line-of-Sight (LoS) link. Secondly, the received optical power at users drops as the angle of irradiance between a LED lamp and the user increases, imposing a range constraint on the VLC nodes. So, inspired by the *Art Gallery Problem*, we optimize the number and the locations of VLC nodes by characterizing the PV graph as a dual presentation of the floor plan and a *Maximal Clique Clustering* algorithm, which is able to solve not only the art gallery problem but also to extend the approach for the *range constrained* case.**

***Index terms*—** Visible Light Communications; Network Planning; Irregular floor plan; Art gallery problem; Visibility graph; Line-of-Sight; Indoor coverage.

I. Introduction

Following the trend initiated with 5G New Radio (NR), the Sixth Generation (6G) of mobile networks is expected to continue its development towards the incorporation of new Radio Frequency (RF) bands beyond Millimeter-Wave bands, wider communication bandwidths, and even denser deployments of small cells [1]. VLC is a potential technology to achieve some of these target goals, taking advantage of the ubiquitous presence of LED lamps to enable an ultra-dense deployment of wireless access nodes [2]. Compared to RF [3], VLC is a strong technology candidate for secure, private, safe, low-cost, and license-free communications within the 6G landscape. As a distinctive characteristic, VLC signals cannot propagate through opaque obstacles such as walls and curtains. Although this feature restricts a good indoor service coverage, it can also be considered as an advantage to enable secured communications or increase the density of VLC cells by confining the light signal into the designated service area.

VLC networks should be planned to provide seamless coverage indoors [4]. Most of the research done so far in the literature has considered a deployment of nodes to enable a regular tessellation of cells in a small [5] or (infinitely) large room [6] environment, aiming at mitigating the inter-cell interference. However, the service floor layouts in VLC networks are not necessarily as regular as squares or rectangles. This problem becomes relevant when LoS link needs to be ensured in the whole floor plan [7], since the power of the reflected light beams from the walls, floor, and even furniture is much weaker than the one of the LoS beam between the VLC node and its terminal [8]. When the shape of the indoor environment becomes irregular, the most convenient way to deploy the minimum number of VLC nodes for reliable communication services has not been studied in detail so far.

The art gallery problem, raised by Victor Klee in 1973, aims at minimizing the number of omni-directional camera guards to fully cover a given floor plan, determining as well their locations [9], [10]. Generally, the art gallery problem is NP-hard. However, Chvatal proposed the upper bound of $\lfloor n/3 \rfloor$ guards, where n is the number of layout vertices [11]. Furthermore, placing one guard in all reflex vertices of the layout is enough and sometimes necessary for full coverage [12]. Specifically, given an orthogonal layout, wherein each edge of the layout is horizontal or vertical, only $\lfloor n/4 \rfloor$ guards suffices [13]. To our best knowledge, the most accurate solution to solve this problem uses an algebraic-based algorithm, wherein the vertices of the grid are iteratively weighted [14]. However, the literature lacks analytical methods to optimize indoor placements that consider range constraints of guards.

Similar to camera guards in art gallery problem, LED lamps are also obstructed by the presence of physical obstacles. However, the effective propagation range constraint due to the limited SNR in the VLC link has not been studied in the art gallery problem. The main novelty of this paper initially lies in the modeling of the art gallery problem with the problem of maximal clique clustering in a visibility graph modeling as a dual presentation of the floor plan. Interestingly, the structure of the proposed visibility graph modeling enables to take into account the range constraint, wherein all the points in the layout are not only visible from, but also in the range of at least one VLC node[1]. As a result, the placement for the smallest set of VLC nodes is derived. Though there are similarities between the placement of VLC nodes to provide

This research work was partly supported by Academy of Finland under the grant 339446.

[1] In this paper, the terms *guard* and *VLC node* are used interchangeably.

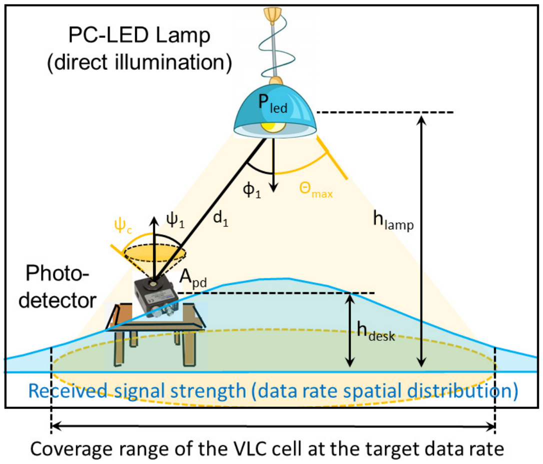

Fig. 1. Indoor VLC cell including a white LED lamp with direct illumination. Blue (Gaussian-like) spatial distribution of the optical power determines the coverage range ($2\,r$) that guarantees the target data rate on the cell edge.

data and illumination services, there are also key differences between both network planning problems. That is, for VLC data service planning, it is usually required that a minimum data rate is guaranteed for those terminals that lie in the cell-edge areas of the multi-cell network. On the other hand, when the objective is to optimize the deployment of the nodes for illumination purposes, the aim is to guarantee a minimum mean illumination and a target level of illumination uniformity on the whole service area of the VLC network [6].

The rest of the paper is structured as follows. Section II describes VLC network planning problem statement. Section III presents the proposed methods and Section IV provides simulation results. Finally, conclusions are drawn in Section V.

II. VLC Network Planning Problem Statement

The fundamentals of VLC planning that justify the use of the Art Gallery problem approach are presented in this section.

A. Coverage range of the VLC cell

Different channel models have been proposed in the literature to characterize the indoor propagation of VLC signals. This paper focuses on the *direct illumination* case [7], where the effect of reflections on walls, floor, and/or other obstacles that may be present in the room are neglected (see Fig. 1).

Let us assume that the Phosphor-Converted (PC)-LED is modeled as a source of light with a Lambertian radiation pattern; then, the DC gain of the optical channel between the LED transmitter and the Photodetector (PD) receiver is [15]

$$H_{\mathrm{led,pd}}^{\mathrm{dir}}(0)=\begin{cases}\frac{(m+1)A_{\mathrm{pd}}}{2\pi {d_1}^2}\cos^m(\phi_1)\cos(\psi_1), & 0\le\psi_1\le\Psi_{\mathrm{c}},\\ 0, & \psi_1>\Psi_{\mathrm{c}},\end{cases} \tag{1}$$

where m denotes the Lambert index of the PC-LED, A_{pd} [m^2] is the physical area of the PD, ϕ_1 [rad] and ψ_1 [rad] refer to the angle of irradiance and incidence of the LoS link, respectively.

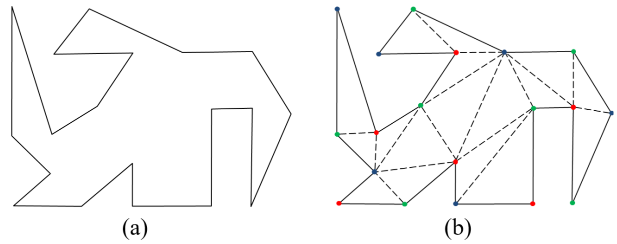

Fig. 2. a) A given layout [9]. b) Layout triangulation and 3-coloring methods.

Also, d_1 [m] is the distance between transmitter and receiver, and Ψ_{c} [rad] is the Field of View (FOV) semi-angle of the PD. In practice, the Lambert index of the LED can be computed from $m=-1/\log_2\left[\cos(\theta_{\max})\right]$, where $\theta_{\max}$ [rad] defines the source radiation semi-angle at half power of the PC-LED.

Finally, the spectral optical power of the light that reaches the PD at wavelength λ is given by

$$p_{\mathrm{o,pd}}^{\mathrm{dir}}(\lambda)=P_{\mathrm{led}}\,H_{\mathrm{led,pd}}^{\mathrm{dir}}(0)\,S_{\mathrm{o}}^{(\mathrm{w})}(\lambda), \tag{2}$$

where P_{led} [W] and $S_{\mathrm{o}}^{(\mathrm{w})}(\lambda)$ are the total radiant power and spectral power distribution of the PC-LED, respectively.

The DC current at the output of the PD is given by

$$i_{\mathrm{pd}}^{\mathrm{dir}}(0)=\int_{\lambda_{\mathrm{l}}}^{\lambda_{\mathrm{u}}} p_{\mathrm{o,pd}}^{\mathrm{dir}}(\lambda)\,\mathrm{R}_{\mathrm{pd}}(\lambda)\,f_{\mathrm{o}}(\lambda)\,d\lambda, \tag{3}$$

where $\mathrm{R}_{\mathrm{pd}}(\lambda)$ [A/W] is the responsivity of the PD and $f_{\mathrm{o}}(\lambda)$ is the transmitance of the optical passband filter with lower (λ_{l}) and upper (λ_{u}) cutoff wavelengths. The ambient light that is present in the room, as well as the instantaneous power of the data-carrying signal that reaches the PD, generate shot noise with Root Mean Square (RMS) value v_{n} that is added on top of the thermal noise that is introduced by the Transimpedance Amplifier (TIA) with gain G_{tia} embedded into the PD.

Hence, the SNR at the output of the PD is given by

$$\Gamma_{\mathrm{pd}}(0)=\left|\left(i_{\mathrm{pd}}^{\mathrm{dir}}(0)\,G_{\mathrm{tia}}\right)/v_{\mathrm{n}}\right|^2. \tag{4}$$

Accordingly, the cell radius of the VLC node is determined such that the received SNR on the cell range is high enough to guarantee the target data rate in the whole service area. In case of overlap between the adjacent cells, Joint Coordinated Multi-Point (CoMP) can further increase the data rate [5].

B. Art Gallery Problem

The art gallery problem aims at placing a minimum number of stationary omni-directional camera guards to cover all the points of an art gallery with an arbitrary layout [9], [10]. We picture the walls of the art gallery as a layout with n vertices. For instance, one guard anywhere in a convex layout suffices for full coverage, as every point inside or on the convex polygon is openly visible from any other point in it. Generally, minimizing the number of guards to cover a layout is a NP-hard problem. However, *Chvatal Theorem* determines an upper-bound to the minimum number of guards.

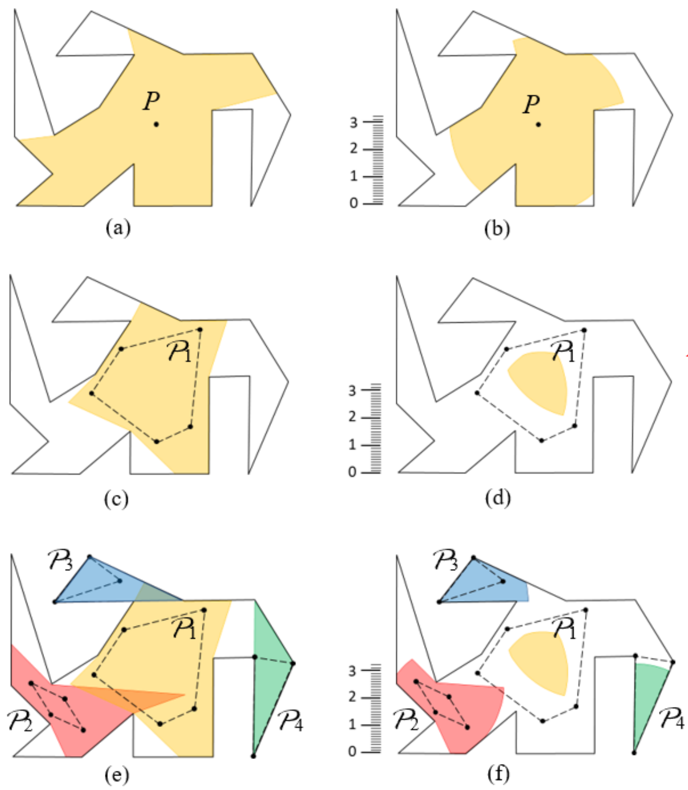

Fig. 3. Visibility area(s) for: a) point P; b) point P with range constraint; c) polygon $\mathcal{P}_1$; d) polygon $\mathcal{P}_1$ with range constraint; e) four polygons $\mathcal{P}_1$,..., $\mathcal{P}_4$; f) four polygons $\mathcal{P}_1$,..., $\mathcal{P}_4$ with range constraint.

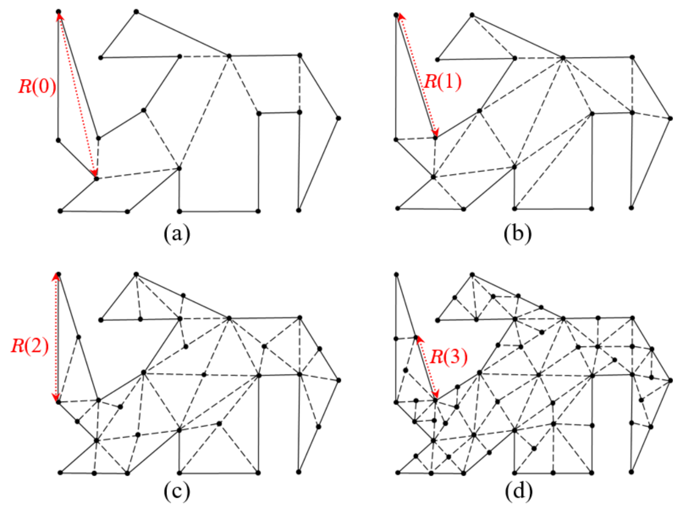

Fig. 4. Convex partitioning methods. a) MCP or equivalently 0-order triangulation. b) Triangulation or equivalently 1-order triangulation. c) 2-order triangulation. d) 3-order triangulation.

Chvatal's Theorem. *To fully cover any layout with n vertices, $\lfloor n/3 \rfloor$ guards are sufficient and occasionally necessary.*

Fisk proof. The theorem is proven by Fisk proof showing the vertices of every layout are 3-colorable [16]. A layout can be partitioned into a set of triangles in a polynomial time, known as *triangulation* algorithm [9]. Then, we can start coloring vertices of a triangle in the layout by three different colors, let us say red, blue, and green. Then, we continue coloring single uncolored vertices of adjacent triangles iteratively, such that no adjacent vertices have the same color. As a result, all the triangles have all three colors on their vertices. Since placing a set of guards at any specific color vertices sees all the triangles, deploying guards on the vertices with the minimum number of colors, i.e. $\lfloor n/3 \rfloor$, suffices to cover the layout. On the other hand, exactly $\lfloor n/3 \rfloor$ guards are necessary to cover a *comb* shape layout [9], [10]. Thus, Chvatal's theorem follows. □

Fisk proof is visualized in Fig. 2 for a given layout with $n = 19$ vertices. First, the layout is partitioned into $n - 2 = 17$ triangles via the triangulation method. Then, 3-coloring the vertices results in different colors at each vertex. So, deploying $\lfloor n/3 \rfloor = 6$ guards on red vertices covers the whole layout.

Generally, Chvatal theorem fails to minimize the number of guards to cover a layout. For instance, a convex layout needs only one guard for full visibility, even with large n. Also, the minimum number of guards does not necessarily locate on the vertices, such as in star-shaped layouts, wherein only one guard in the middle may suffice. Moreover, the theorem does not take into account range constraints, such as the ones imposed by VLC nodes.

III. Proposed Method

In this section, we revisit the art gallery problem by proposing a PV graph modeling to not only minimize the number of guards and to find their locations in any layout, but also to add compatibility to range requirements in VLC networks. To this end, we express several definitions to support the PV graph modeling. Assuming that X and P denote two points inside or on the layout, we characterize the following two definitions.

Definition 1. Visibility Area of a Point. X is inside the visibility area of P, indicated by $X \in \mathcal{V}(P)$, if and only if:

- The line segment XP is entirely inside the layout, and
- $\|XP\| \leq r$, wherein r denotes the maximum range.

In other words, $X \in \mathcal{V}(P)$ if there is no layout edge to block the LoS between P and X, and simultaneously, X is within the range of P[2]. Furthermore, we extend Definition 1 to a polygon $\mathcal{P}$ with l vertices inside or on the layout.

Definition 2. Visibility Area of a Polygon. X is inside the visibility area of $\mathcal{P}$, indicated by $X \in \mathcal{V}(\mathcal{P})$, if and only if X is visible from all its vertices $P_1, P_2, ..., P_l$.

From Definitions 1 and 2, we can immediately conclude that $\mathcal{V}(\mathcal{P}) = \mathcal{V}(P_1) \cap \mathcal{V}(P_2) ... \cap \mathcal{V}(P_l)$. Figure 3 visualizes visibility

[2]The unconstrained $\mathcal{V}(P)$ is equivalent to the $\mathcal{V}(P)$ with range constraint $r = \infty$. So hereafter, we remove the term *unconstrained*.

areas in Definitions 1 and 2. In Fig. 3a), the yellow area displays $\mathcal{V}(P)$, while in Fig. 3b), the yellow area represents the $\mathcal{V}(P)$ with maximum $r = 3.2$ units. On the other hand, the yellow area in Fig. 3c) represents $\mathcal{V}(\mathcal{P}_1)$, the visibility area for the irregular pentagon $\mathcal{P}_1$ and Fig. 3d) illustrates $\mathcal{V}(\mathcal{P}_1)$ with maximum $r = 3.2$ units. Also the red, blue, and green areas in Fig. 3e) display $\mathcal{V}(\mathcal{P}_2)$, $\mathcal{V}(\mathcal{P}_3)$, and $\mathcal{V}(\mathcal{P}_4)$, respectively. For example, it can be observed that $\mathcal{V}(\mathcal{P}_1) \cap \mathcal{V}(\mathcal{P}_2) \neq \emptyset$ and $\mathcal{V}(\mathcal{P}_2) \cap \mathcal{V}(\mathcal{P}_3) = \emptyset$. In Fig. 3f), the same colors are used to indicate $\mathcal{V}(\mathcal{P}_1)$, ... , $\mathcal{V}(\mathcal{P}_4)$, respectively, with $r = 3.2$ units. It is observed here that the range constrained visibility areas are all disjoint, $\mathcal{V}(\mathcal{P}_i) \cap \mathcal{V}(\mathcal{P}_j) = \emptyset$ for $i, j = 1, ..., 4$ and $i \neq j$.

Now, to systematically partition the layout to convex polygons, we express Definitions 3 and 4.

Definition 3. Maximal Convex Partitioning (MCP) refers to adding a minimum number of diagonals to a layout such that all the resulting polygons are convex.

MCP methods are not unique and they can be performed via different algorithms, such as adding non-intersecting diagonals to the reflex vertices of the layout until there is no polygon with reflex vertices left. Another algorithm is via layout triangulation and removing the diagonals randomly as long as all the polygons remain convex. However, we occasionally need smaller polygons to guarantee the coverage or to find a smaller set of nodes to cover the whole layout. Since a triangle is always a convex polygon, we make the following definition.

Definition 4. $\mathbf{m}$ – order Triangulation is a m-step triangle partitioning method for $m \geq 1$, connecting the mid-point of the largest side of all triangles to the opposite vertex.

Fig. 4 exhibits the convex partitioning and triangularization methods. Fig. 4a) presents an MCP[3] example with 8 convex polygons and Fig. 4b) displays the triangulation. Then, connecting the midpoint of the largest side at each triangle to the opposite vertex in Fig. 4b), we derive the 2-order triangulation shown in Fig. 4c). Performing the same procedure on 2-order triangulation, we derive the 3-order triangulation in Fig. 4d).

Remark 1. A m-order triangulated layout with $m \geq 1$ is consisted of $M = (n - 2) \times 2^{m-1}$ triangles.

Now, we define $R(0)$ as the maximum distance between polygon vertices in MCP method and $R(m)$, for $m \geq 1$, as the maximum triangle side length in m-order triangulation through all the polygons.

Remark 2. In any partitioned layout, the maximum triangle side length $R(m)$ is decreasing with m.

Then, we characterize the visibility to a triangle area.

[3] To preserve the consistency of the symbols, MCP method is interpreted as 0-order triangulation.

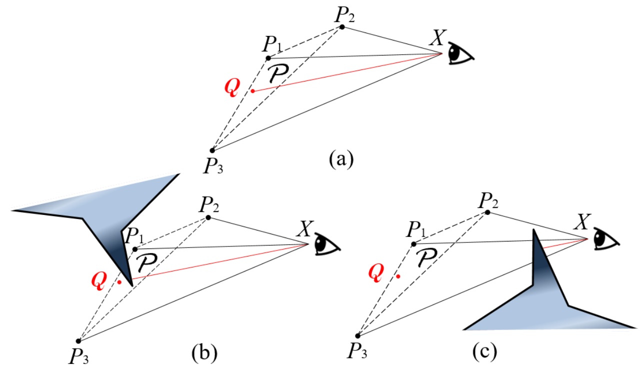

Fig. 5. Visibility between point X and triangle $\mathcal{P}$ with a point Q inside. a) No obstacle. b) Layout edge intersects the XQ and one of the triangle sides. c) Layout edge intersects XQ and XP_i for some i.

Lemma 1. Assume $\mathcal{P}$ denotes a triangle from m-order triangulated *layout with no holes*[4] and with vertices P_1, P_2, and P_3 as in Fig. 5a). If the point $X \in \mathcal{V}(\mathcal{P})$, then for any point Q inside $\mathcal{P}$ or on its sides, $X \in \mathcal{V}(Q)$.

Proof. From Definition 4 and since $X \in \mathcal{V}(\mathcal{P})$ and Q is inside or on $\mathcal{P}$, both X and Q are inside or on the layout. Firstly, the farthermost point of a triangle to any point on the plane is one of the vertices and thus, $\|XQ\| \leq \max(\|XP_1\|, \|XP_2\|, \|XP_3\|) \leq r$. Secondly, we prove that no layout edge intersects the segment XQ. To show the contradiction, we assume that an edge intersects XQ. Since the whole XQ lies inside the convex hull of the union of $\mathcal{P}$ and X, the blocking edge also intersects at least one of the convex hull boundaries, i.e., a side of $\mathcal{P}$ as in Fig. 5b), or the segment XP_i for some i as in Fig. 5c). Intersecting a triangle side contradicts the definition of m-order triangulation and intersecting one of the segments XP_1, XP_2, or XP_3 contradicts $X \in \mathcal{V}(\mathcal{P})$. Hence, Lemma 1 follows. $\square$

Lemma 1 implies that placing a set of guards inside the convex partitioned layout, such that there is at least one guard in the visibility area of each polygon, covers the whole layout.

So, Remark 2 and Lemma 1 yield the following remark.

Remark 3. To guarantee full coverage of all triangles from their visibility areas, we increase the order of triangulation to satisfy $R(m) < r$. On the other hand, increasing m increases the probability to find the smallest set of guards to cover the whole layout in the cost of higher complexity.

Denoting M as the number of polygons in the layout, we define a visibility graph modeling as follows.

Definition 5. Partition–based Visibility (PV) Graph refers to an indirect unweighted graph consisting of M nodes, representing the polygons (triangles) of the layout $\mathcal{P}_1$, ..., $\mathcal{P}_M$.

[4] Layouts with holes are beyond the scope of this paper.

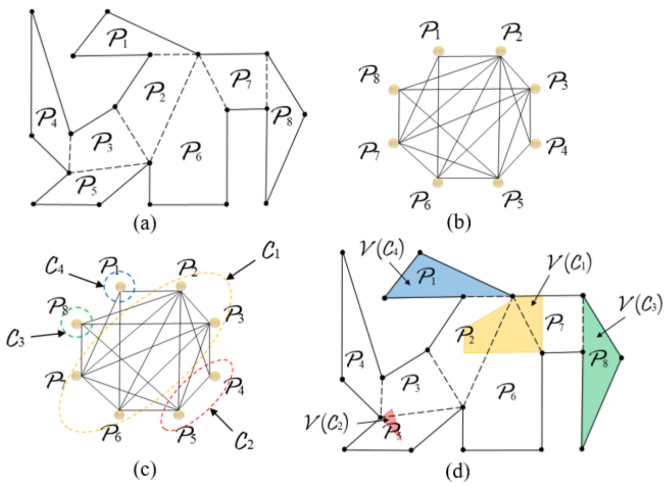

Fig. 6. PV graph and a non-optimal clique partitioning. a) The layout partitioned by MCP method. b) PV graph associated to the partitioned layout. c) A non-optimal clique partitioning for the PV graph. d) Visibility sub-areas for the cliques in the non-optimal clique partitioning.

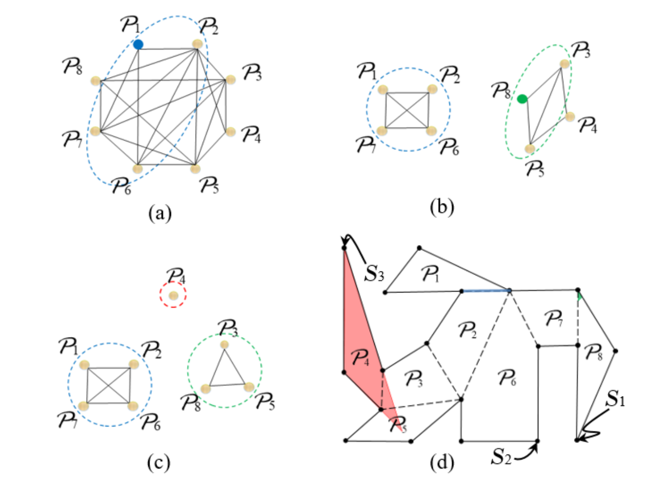

Fig. 7. Optimal guard placement via maximal clique clustering steps. a) The PV graph shown in Fig. 6b) marked with a largest clique. b) The remaining graph marked with next largest clique. c) A single node as a largest clique in the remaining graph. d) Visibility sub-areas for the three cliques in Fig. 7c).

Two nodes $\mathcal{P}_i$ and $\mathcal{P}_j$ in the graph are connected with an edge if and only if $\mathcal{V}(\mathcal{P}_i)\cap\mathcal{V}(\mathcal{P}_j) \neq \emptyset$ for $1 \leq i, j \leq M$ and $i \neq j$.

Possible guard placements for a full coverage of the layout are characterized through the following theorem.

Theorem 1. Any partitioning of the PV graph into g cliques, say $\mathcal{C}_1$,..., $\mathcal{C}_g$, results in a set of sub-areas $\mathcal{V}(\mathcal{C}_1)$,..., $\mathcal{V}(\mathcal{C}_g)$ in the layout. Then, deploying one guard anywhere inside each sub-area fully covers the layout.

Proof. Upon the definition, the nodes of each clique do not overlap with other cliques and the union of the nodes in the cliques forms all the nodes of the PV graph $\mathcal{P}_1$,..., $\mathcal{P}_M$.

TABLE I
MAXIMAL CLIQUE CLUSTERING ALGORITHM

Initialization
r: maximum range
$\mathcal{P}_1, ..., \mathcal{P}_M$: polygons in the layout % Remark 3
$\mathcal{G} \leftarrow \mathsf{PVgraph}\big(\mathcal{V}(\mathcal{P}_1), ..., \mathcal{V}(\mathcal{P}_M)\big)$ % Definition 5
While $\mathcal{G} \neq \emptyset$
$[\mathcal{P}_{q_1}, ..., \mathcal{P}_{q_M}] \leftarrow$ Nodes of $\mathcal{G}$ in ascending degrees order
$\mathcal{C} \leftarrow \mathcal{P}_{q_1}$ % Choose the node with minimum degree
For $i = 2 : M$
If $\mathcal{C} \cup \mathcal{P}_{q_i}$ forms a clique & $\mathcal{V}(\mathcal{C} \cup \mathcal{P}_{q_i}) \neq \emptyset$
$\mathcal{C} \leftarrow \mathcal{C} \cup \mathcal{P}_{q_i}$
End If
End For
Deploy a guard anywhere inside $\mathcal{V}(\mathcal{C})$
$\mathcal{G} \leftarrow \mathcal{G} - \mathcal{C}$
$M \leftarrow \lvert\mathcal{G}\rvert$
End While

Assume $\mathcal{C}_k$ with $1 \leq k \leq g$, contains a set of nodes $\mathcal{P}'_{k1}$, $\mathcal{P}'_{k2}$, ..., and $\mathcal{P}'_{k|\mathcal{C}_k|}$. Noting that each node $\mathcal{P}'_{ku}$, $1 \leq k \leq g$ and $1 \leq u \leq |\mathcal{C}_k|$, correspondingly represents a node in the PV graph and consequently a polygon in the layout, we define a visibility sub-area for the clique as $\mathcal{V}(\mathcal{C}_k) = \mathcal{V}(\mathcal{P}'_{k1}) \cap \mathcal{V}(\mathcal{P}'_{k2}) \cap ..., \cap \mathcal{V}(\mathcal{P}'_{k|\mathcal{C}_k|})$. So, from Lemma 1, any point inside $\mathcal{V}(\mathcal{C}_k)$ is visible altogether from any point inside or on the polygons $\mathcal{P}'_{k1}$, $\mathcal{P}'_{k2}$, ..., and $\mathcal{P}'_{k|\mathcal{C}_k|}$. Therefore, deploying g guards, each one anywhere inside $\mathcal{V}(\mathcal{C}_k) \neq \emptyset$ with $1 \leq k \leq g$, fully covers the layout. □

Fig. 6 illustrates a PV graph in an unconstrained case and a clique partitioning. Fig. 6a) shows the layout partitioned to 8 polygons using MCP method and Fig. 6b) depicts its PV graph with 8 nodes. For example, since $\mathcal{V}(\mathcal{P}_5) \cap \mathcal{V}(\mathcal{P}_7) \neq \emptyset$ and $\mathcal{V}(\mathcal{P}_4) \cap \mathcal{V}(\mathcal{P}_6) = \emptyset$, the nodes $\mathcal{P}_5$ and $\mathcal{P}_7$ are connected and the nodes $\mathcal{P}_4$ and $\mathcal{P}_6$ are disconnected. Since a single node is also a clique, we may partition the PV graph into as high as $g = 8$ single node cliques $\mathcal{C}_1$,..., $\mathcal{C}_8$, resulting in highly overlapped sub-areas $\mathcal{V}(\mathcal{C}_k) = \mathcal{V}(\mathcal{P}_k)$ for $1 \leq k \leq 8$. Certainly, deploying 8 guards anywhere inside each of $\mathcal{V}(\mathcal{C}_1)$,..., $\mathcal{V}(\mathcal{C}_8)$ covers the whole layout. To partition the PV graph more efficiently, Fig. 6c) displays a partitioning into $g = 4$ cliques $\mathcal{C}_1$,..., $\mathcal{C}_4$, shown by 4 different colors and the corresponding visibility sub-areas $\mathcal{V}(\mathcal{C}_1)$, ..., $\mathcal{V}(\mathcal{C}_4)$ in Fig. 6d). For instance here, $\mathcal{V}(\mathcal{C}_1) = \mathcal{V}(\mathcal{P}_2) \cap \mathcal{V}(\mathcal{P}_3) \cap \mathcal{V}(\mathcal{P}_6) \cap \mathcal{V}(\mathcal{P}_7)$ and $\mathcal{V}(\mathcal{C}_3) = \mathcal{V}(\mathcal{P}_8)$. So, deploying $g = 4$ guards anywhere inside each sub-area $\mathcal{V}(\mathcal{C}_1)$,..., $\mathcal{V}(\mathcal{C}_4)$ covers the whole layout.

From Theorem 1, art gallery problem can be interpreted as minimizing g in a PV graph. In literature, graph partitioning to the minimum number of cliques refers to a well-known NP-complete problem called *minimum clique cover* [17]. How-

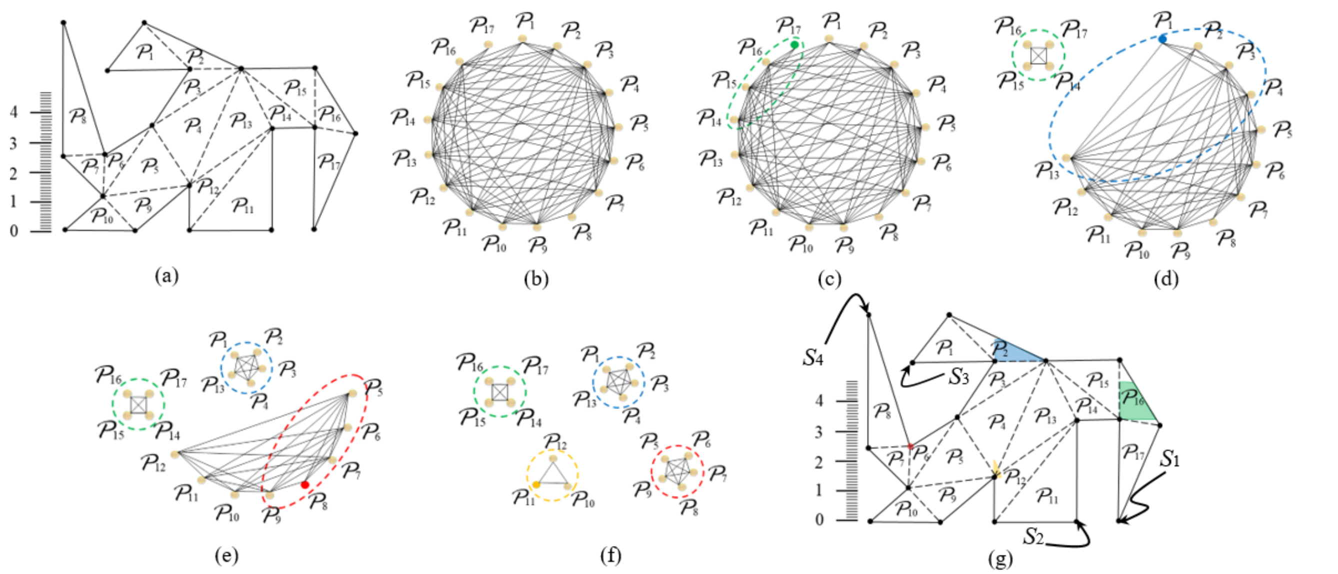

Fig. 8. Optimal guard placement with maximum range $r = 4.7$. a) Layout triangulation. b) PV graph for the triangulated layout, c-f) Maximal clique clustering of the PV graph, g) Visibility sub-areas of the 4 cliques in Fig. 8e).

ever to minimize g, we propose maximal clique clustering algorithm in Table I as follows: I) choose the node $\mathcal{P}_{q_1}$ with minimum degree $d(\mathcal{P}_{q_1})$ in the graph; II) find the largest clique $\mathcal{C}$ that is connected to $\mathcal{P}_{q_1}$ and $\mathcal{V}(\mathcal{C}) \neq \emptyset$; III) deploy a guard in $\mathcal{V}(\mathcal{C})$ and remove all the edges connected to $\mathcal{C}$; IV) start over the algorithm for the remaining graph.

Figure 7 shows the steps of the maximal clique clustering algorithm. Fig. 7a) represents the PV graph in Fig. 6b). Here, $\mathcal{P}_1$ is selected as the node with the minimum degree, and the largest clique connected to $\mathcal{P}_1$ is marked. Removing the clique from the graph, Fig. 7b) shows $\mathcal{P}_8$ as the minimum degree node and the connected largest clique. Subtracting the clique, the remaining graph consists of only one node that is solely clustered as the last clique in Fig. 7c). Finally, Fig. 7d) visualizes the visibility sub-areas for the three cliques in Fig. 7c). So, deploying one guard inside each visibility sub-area results in totally $g = 3$ guards covering the whole layout.

Remark 4. Finding h points S_1, S_2,..., S_h inside or on the layout yields a lower bound to the minimum number of guards, i.e. $h \leq g$, if their visibility areas are pairwise disjoints sets, i.e. $\mathcal{V}(S_i) \cap \mathcal{V}(S_j) = \emptyset$ for $1 \leq i, j \leq h$ and $i \neq j$.

Inspecting Fig. 7d), we find three points S_1, S_2, and S_3 whose visibility areas are pairwise disjoint. Thus from Remark 4, the maximal clique clustering algorithm over the PV graph resulted in the optimal number of guards as $h = g = 3$.

IV. Simulation Results

In this section, we evaluate the performance of the PV graph modeling to optimize the number and the locations of the range constrained VLC nodes. Setting the maximum range $r = 4.7$, Fig. 8 describes the PV graph and the maximal clique clustering steps. Since $R(m = 1) \leq r$ in the convex partitioned layout in Fig. 8a), 1-order triangulation guarantees the coverage for every 17 triangles. Fig. 8b) indicates the PV graph taking into account the visibility areas of the triangles with the maximum range r. Here, the node $\mathcal{P}_{17}$ has the minimum degree and the set of the nodes $\mathcal{P}_{14}$, $\mathcal{P}_{15}$, $\mathcal{P}_{16}$, and $\mathcal{P}_{17}$ form the largest clique connected to $\mathcal{P}_{17}$. So, by cutting off this clique in Fig. 8c), Fig. 8d) finds $\mathcal{P}_1$ as the minimum degree in the remaining graph. Continuing the steps, we end up with 4 cliques in Fig. 8f). Finally, Fig. 8g) illustrates visibility sub-areas for the $g = 4$ cliques, wherein totally 4 guards can be deployed. Additionally, we find $h = 4$ points S_1, S_2, S_3, and S_4 as in Fig. 8g), at which $\mathcal{V}(S_i) \cap \mathcal{V}(S_j) = \emptyset$ with $r = 4.7$ for $1 \leq i, j \leq 4$ and $i \neq j$. As a result from Remark 4, the $h \leq g = 4$ number of guards found in Fig. 8, is optimal.

Fig. 9a) shows the minimum number of VLC nodes that are to cover the layout as a function of the maximum range. It is observed that similar to unconstrained case, setting $r \geq 6.2\,\mathrm{m}$ results in only 3 nodes, whereas setting $r = 4.8$, 3.6 and $2.8\,\mathrm{m}$ results in 4, 5, and 7 VLC nodes, respectively. On the other hand, assuming that the VLC users are randomly distributed in the layout, Fig. 8b) shows the CDF for user distances for the four VLC node layouts with the representative maximum ranges distinguished by colors. It is observed that the deployment of 4 nodes (green curves) outperforms the 3 nodes deployment (red curves) by reducing the 90-th percentile as much as 2 m. Moreover, when deploying 5 nodes (blue curves) and 7 nodes (magenta curves), there is still a decrease in the 90-th percentile, but this gain is much modest than before. Finally, Fig. 10 exhibits the optimal node placements for the representative range constraints. It is seen that setting

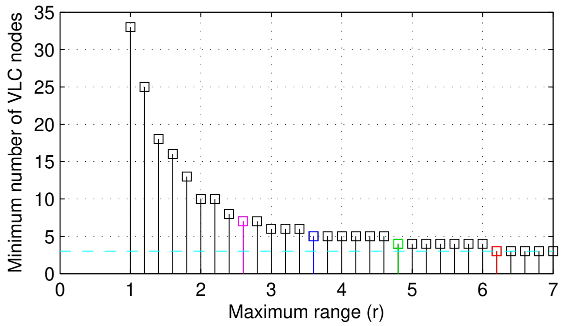

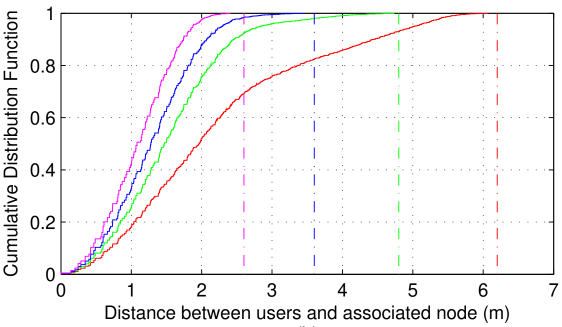

Fig. 9. Effect of maximum range of a VLC node to carry out the network planning: a) Minimum number of VLC nodes to cover the layout for different ranges. b) CDF of user distances to the nearest VLC nodes for 4 representative maximum ranges r (red: 6.2 m; green: 4.8 m; blue: 3.6 m; magenta: 2.6 m).

$r = 6.2$ m results in 3 nodes that are deployed far away. On the other hand, setting $r = 2.6$ m gives 7 closer nodes. Note that these obtained cell radius values are aligned with the ones reported in the literature for optical wireless cellular networks implemented with the cells of the same shape and size, deployed to provide service in large-sized areas [6], [18].

V. Conclusions

We studied indoor VLC network planning in case of an arbitrary floor plan. Starting from the unconstrained art gallery problem, an algorithm was derived to find the minimum number of VLC nodes as well as their locations in order to serve the target area. Apart from the exact locations of the VLC nodes, which are not easy to determine in such a setting, we showed that increasing notably the number of VLC nodes does not provide much more gain in the 90-th percentile of the VLC link distance, which is inversely proportional to the achievable data rate. This gain is even more modest when we focus on the median distance to the nearest VLC node.

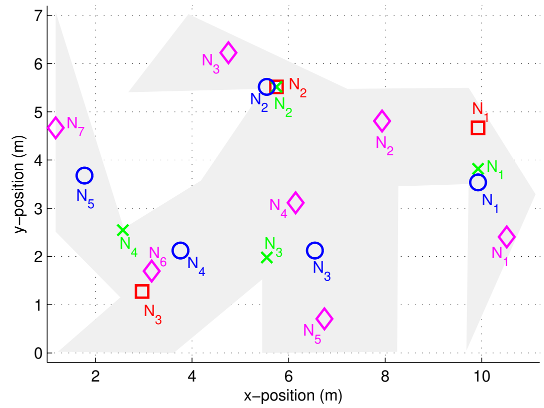

Fig. 10. VLC nodes placements in the layout for different maximum ranges r (red: 6.2 m; green: 4.8 m; blue: 3.6 m; magenta: 2.6 m).

References

[1] W. Jiang, B. Han, M. Habibi, and H. Schotten, "The road towards 6G: A comprehensive survey," *IEEE Open J. Commun. Society*, vol. 2, pp. 334–366, Feb. 2021.

[2] N. Chi, Y. Zhou, Y. Wei, and F. Hu, "Visible light communication in 6G: Advances, challenges, and prospects," *IEEE Veh. Tech. Mag.*, vol. 15, pp. 93–102, Dec. 2020.

[3] D. Karunatilaka, F. Zafar, V. Kalavally, and R. Parthiban, "LED based indoor visible light communications: State of the Art," *IEEE Commun. Surv. & Tut.*, vol. 17, pp. 1649–1678, 3Q 2015.

[4] H. Haas, L. Yin, Y. Wang, and C. Chen, "What is LiFi?," *J. Lightwave Tech*, vol. 34, pp. 1533–1544, Mar. 2016.

[5] A. Dowhuszko and A. Pérez-Neira, "Achievable data rate of coordinated multi-point transmission for visible light communications," in *Proc. IEEE Int. Symp. Personal Indoor and Mobile Radio Commun.*, pp. 1–7, Oct. 2017.

[6] B. Genovés Guzmán, A. Dowhuszko, V. Gil Jiménez, and A. Pérez-Neira, "Resource allocation for cooperative transmission in optical wireless cellular networks with illumination requirements," *IEEE Trans. Commun.*, vol. 68, pp. 6440–6455, Oct. 2020.

[7] A. Dowhuszko, M. Ilter, and J. Hämäläinen, "Visible light communication system in presence of indirect lighting and illumination constraints," in *Proc. IEEE Int. Conf. Commun.*, pp. 1–6, June 2020.

[8] C. Chen, D. Basnayaka, and H. Haas, "Downlink performance of optical attocell networks," *J. Lightwave Tech.*, vol. 34, pp. 137–156, Jan. 2016.

[9] M. De Berg, M. Van Kreveld, M. Overmars, and O. Schwarzkopf, "Computational geometry," in *Computational geometry*, pp. 1–17, Springer, 1997.

[10] M. Aigner, G. M. Ziegler, K. H. Hofmann, and P. Erdos, *Proofs from the Book*, vol. 274. Springer, 2010.

[11] M. Giaquinto, "Mathematical proofs: The beautiful and the explanatory," *Journal of Humanistic Mathematics*, vol. 6, no. 1, pp. 52–72, 2016.

[12] J. O'rourke *et al.*, *Art gallery theorems and algorithms*, vol. 57. Oxford University Press Oxford, 1987.

[13] J. Kahn, M. Klawe, and D. Kleitman, "Traditional galleries require fewer watchmen," *SIAM Journal on Algebraic Discrete Methods*, vol. 4, no. 2, pp. 194–206, 1983.

[14] A. Efrat and S. Har-Peled, "Guarding galleries and terrains," *Information processing letters*, vol. 100, no. 6, pp. 238–245, 2006.

[15] T. Komine and M. Nakagawa, "Fundamental analysis for visible-light communication system using LED lights," *IEEE Trans. Consumer Electronics*, vol. 50, pp. 100–107, Feb. 2004.

[16] S. Fisk, "A short proof of chvátal's watchman theorem," *Journal of Combinatorial Theory, Series B*, vol. 24, no. 3, p. 374, 1978.

[17] R. M. Karp, "Reducibility among combinatorial problems," in *Complexity of computer computations*, pp. 85–103, Springer, 1972.

[18] B. Genovés Guzmán, A. A. Dowhuszko, V. P. Gil Jiménez, and A. I. Pérez-Neira, "Robust cooperative multicarrier transmission scheme for optical wireless cellular networks," *IEEE Photonics Technology Letters*, vol. 30, pp. 197–200, Jan. 2018.